

complex. By using  $\lambda_{12} = 1.0$  eV and taking  $\lambda_{22}$  for Ru(bpy)<sup>2+/3+</sup> self-exchange reaction to be 0.53 eV,<sup>27,28</sup> the reorganization energy  $\lambda_{11}$  for the cyt-c<sup>2+</sup>/cyt-c<sup>3+</sup> self-exchange reaction can be estimated from the additivity rule of Marcus<sup>4</sup> to be 1.5 eV. Another system which is related to the present one is the (ZnP,Fe<sup>3+</sup>P) hybrid hemoglobin,<sup>30,31</sup> the reorganization energy  $\lambda_{12}$  of which for intramolecular electron transfer between the two metalloporphyrins has been determined recently to be about 2.3 eV.<sup>31</sup> The large difference (1.0 vs. 2.3 eV) found for the two systems may arise from the presence of an additional protein subunit in the hybrid hemoglobin, and/or that hemoglobin has an intrinsically large  $\lambda_{12}$  because it is not designed to carry out electron-transfer

function. Further work along this line involving more proteins will be required before a more definite answer can be reached. Preliminary evidences also indicate that the transfer rate for the hybrid hemoglobin exhibits a much stronger  $\Delta E$  dependence than what is presently observed within the same  $\Delta E$  range.<sup>31</sup> This difference is not unexpected in view of the large  $\lambda_{12}$  found for the (ZnP,Fe<sup>3+</sup>P) hybrid.

In conclusion, this work has demonstrated the usefulness of the porphyrin system in the study of the electron-transfer processes in proteins. Two transfer rates can be determined for each porphyrin as it goes through the P → P\* → P<sup>+</sup> → P cycle following the absorption of a photon. In the future, we hope to study several other proteins over a wide  $\Delta E$  range in order to gain more insight into the electron-transfer mechanism in biological systems.

**Registry No.** ZnTPPS, 80004-36-0; ZnTPPC, 83294-30-8; ZnTMPyP, 40603-58-5; H<sub>2</sub>TPPS, 39174-47-5; H<sub>2</sub>TMPyP (chloride salt), 92739-63-4; CH<sub>2</sub>TMPyP, 38673-65-3; Zn(TPyP), 31183-11-6; H<sub>2</sub>TPyP, 16834-13-2; cyt-c, 9007-43-6.

- (28) Siders, P.; Marcus, R. A. *J. Am. Chem. Soc.* **1981**, *103*, 741-747.  
 (29) Marcus, R. A. *J. Chem. Phys.* **1965**, *43*, 679-701.  
 (30) McGourty, J. L.; Blough, N. V.; Hoffman, B. M. *J. Am. Chem. Soc.* **1983**, *105*, 4470-4472.  
 (31) Peterson-Kennedy, S. E.; McGourty, J. L.; Hoffman, B. M. *J. Am. Chem. Soc.* **1984**, *106*, 5010-5012.

## Infrared Multiphoton Isomerization Reactions of Alkenes and Dienes

Frederick D. Lewis,\* Peter Teng, and Eric Weitz\*

Contribution from the Department of Chemistry, Northwestern University, Evanston, Illinois 60201. Received August 22, 1985

**Abstract:** The infrared multiphoton laser-induced unimolecular isomerization reactions of several simple alkenes, conjugated alkenes, and pentadienes have been investigated. Excitation of (*E*)-2-butene, pentene, and hexene results in contrathermodynamic *E* → *Z* isomerization and fragmentation, the isomerization/fragmentation ratio decreasing with increasing chain length and increasing laser fluence. These results are in qualitative agreement with RRKM calculations for average reactant energies of 75-85 kcal/mol. In addition to products of C-C homolysis observed with all three alkenes, 1-butene and 1,3-butadiene are formed from (*E*)-2-butene. (*E*)-Crotononitrile undergoes laser-induced isomerization without fragmentation, resulting in quantitative conversion to the *Z* isomer. In contrast, (*E*)-methyl crotonate undergoes both isomerization and fragmentation, while (*E*)-ethyl crotonate undergoes essentially quantitative elimination of ethylene. Irradiation of (*E*)- or (*Z*)-1,3-pentadiene at low laser fluences results exclusively in *E* ⇌ *Z* isomerization resulting in steady-state isomer ratios which depend upon the relative magnitude of the single photon cross sections of the two isomers. At higher fluences, both isomers are converted to cyclopentadiene and trace amounts of 1,4-pentadiene. Irradiation of 1,4-pentadiene results in efficient isomerization to (*E*)- and (*Z*)-1,3-pentadiene which reacts further to yield cyclopentadiene. The factors which govern these and related infrared multiphoton reactions are discussed.

The availability of high-powered pulsed infrared lasers has led to renewed interest in the unimolecular isomerization reactions of unsaturated hydrocarbons within the last decade.<sup>1</sup> The results of pulsed infrared multiphoton (IRMP) excitation of unsaturated hydrocarbons can differ markedly from those of conventional heating. Among the significant achievements of the IRMP method are (a) contrathermodynamic isomerization in a two-isomer system (*A* ⇌ *B*),<sup>2-4</sup> (b) trapping of kinetically labile intermediates in consecutive reactions (*A* → *B* → *C*),<sup>5,6</sup> and control of branching

ratios in competing reactions (*A* → *B* + *C*).<sup>7,8</sup> These achievements are based on the wavelength selectivity and rapid heating provided by pulsed infrared lasers. Pulsed excitation of *A* under collision-free conditions at a frequency where *B* absorbs less strongly than *A* allows the formation of *B* even when it is less stable than *A* (contrathermodynamic) or *C* (trapping of kinetically labile intermediates). In cases where the product-forming channels have different activation energies and preexponential factors, the average energy of vibrationally excited *A* can be altered by varying the laser fluence, thereby changing the ratio of products *B* and *C* in competing reactions.

(1) (a) Lewis, F. D.; Buechele, J. L.; Teng, P. A.; Weitz, E. *Pure Appl. Chem.* **1982**, *54*, 1683. (b) Lewis, F. D.; Weitz, E. *Acc. Chem. Res.* **1985**, *18*, 188.

(2) (a) Yogev, A.; Glatt, I. *J. Am. Chem. Soc.* **1976**, *98*, 7087. (b) Yogev, A.; Benmair, R. M. *Chem. Phys. Lett.* **1977**, *46*, 290.

(3) (a) Buechele, J. L.; Weitz, E.; Lewis, F. D. *J. Am. Chem. Soc.* **1981**, *103*, 3588. (b) Buechele, J. L.; Weitz, E.; Lewis, F. D. *J. Chem. Phys.* **1982**, *77*, 3500.

(4) Teng, P. A.; Weitz, E.; Lewis, F. D. *J. Am. Chem. Soc.* **1982**, *104*, 5518.

(5) Nguyen, H. H.; Danen, W. C. *J. Am. Chem. Soc.* **1981**, *103*, 6253.

(6) Lewis, F. D.; Teng, P. A.; Weitz, E. *J. Phys. Chem.* **1983**, *87*, 1666.

(7) (a) Mao, C.-R.; Presser, N.; John, L.-S.; Moriarty, R. M.; Gordon, R. *J. Am. Chem. Soc.* **1981**, *103*, 2105. (b) Farneth, W. E.; Thomsen, M. W.; Schultz, N. L.; Davies, M. A. *J. Am. Chem. Soc.* **1981**, *103*, 2105. (c) Danen, W. C.; Rio, V. C.; Setser, D. W. *J. Am. Chem. Soc.* **1982**, *104*, 5431. (d) Setser, D. W.; Nguyen, H. H.; Danen, W. C. *J. Phys. Chem.* **1983**, *87*, 408.

(8) (a) Buechele, J. L.; Weitz, E.; Lewis, F. D. *J. Am. Chem. Soc.* **1979**, *101*, 3700. (b) Buechele, J. L.; Weitz, E.; Lewis, F. D. *J. Phys. Chem.* **1984**, *88*, 868.

Table I. Frequency and Fluence Dependence of per Pulse Yields of Alkene *E* to *Z* Isomerization

alkene	$\nu_{\text{ex}}$ , cm <sup>-1</sup>	$10^{19}\sigma_E$ , cm <sup>2</sup> a	$10^{19}\sigma_Z$ , cm <sup>2</sup> a	fluence, J/cm <sup>2</sup>	$10^5(\text{yield}/\text{pulse})^{b,c}$ <i>E</i> → <i>Z</i>
2-butene	953	0.69	0.10	3.4	N.R.
	969	1.10	0.38	3.9	110
	975	1.02	0.50	3.4	14.5
2-pentene	953	1.00	0.05	3.2	17
				3.5	44
	969	1.09	<0.01	3.5	48
				3.8	61
				4.0	111
2-hexene	975	0.8	<0.01	3.4	9
				3.6	N.R.
	953	0.70	0.06	3.6	20
				4.0	110
				3.7	25
crotonitrile	931	0.64	0.09	2.0	11
				3.0	40
				3.2	70
				3.5	90
methyl crotonate	978	0.45	0.04	3.4	80
				3.4	80
	975	10		0.8	1
				1.0	4
				1.3	4.5
				1.4	9
				1.5	13
				1.7	14

<sup>a</sup>Single photon cross sections obtained from infrared absorption spectrum ( $\pm 10\%$ ). <sup>b</sup>Yield of molecules in irradiated volume converted per pulse at low conversions ( $<5\%$ ). <sup>c</sup>Reaction of *Z* isomers was not observed at reported  $\nu_{\text{ex}}$ .

We have previously reported the IRMP-induced contrathermodynamic isomerization of 2-methyl- and 2,3-dimethylbutadiene to methylcyclobutenes.<sup>3</sup> While these reactions are substantially endothermic ( $\Delta H \sim 10$  kcal/mol), their activation energies ( $E_a \sim 46$  kcal/mol) are sufficiently low to allow IRMP isomerization to occur without significant competition from higher energy fragmentation pathways. In contrast, our preliminary experiments on the IRMP reactions of (*E*)-2-butene indicated that fragmentation competes with mildly endothermic *E* → *Z* (trans to cis) isomerization ( $\Delta H = 1.04$  kcal/mol).<sup>4</sup> The high activation energy for the isomerization process ( $E_a = 63$  kcal/mol) requires the use of laser fluences sufficiently high for fragmentation reactions to occur. We report here our investigations of the IRMP reactions of several linear (*E*)-2-alkenes,  $\alpha,\beta$ -unsaturated nitriles and esters, and pentadienes. The results serve to extend and define the scope of IRMP contrathermodynamic *E* → *Z* isomerization reactions and to elucidate the competing isomerization and fragmentation reaction pathways of these molecules. Of special interest is the previously unobserved unimolecular isomerization of 1,4-pentadiene to (*E*)- and (*Z*)-1,3-pentadienes.

## Results

**Infrared Multiphoton Irradiation.** Standard irradiation conditions employed the collimated output of a tunable pulsed CO<sub>2</sub> laser to excite samples of alkene or diene (0.1-torr initial cell pressure) at room temperature ( $21 \pm 1$  °C). These conditions have previously been shown to provide essentially collision-free excitation of unsaturated hydrocarbons and to minimize fragmentation due to local heating, dielectric breakdown, or wall effects.<sup>3</sup>

**Reactions of 2-Alkenes.** (*E*)-Alkenes possess moderately strong absorption bands at 950–1000 cm<sup>-1</sup> due to CH=CH out-of-plane deformation of the hydrogen atoms attached to the double bond.<sup>9</sup> (*Z*)-Alkenes absorb only weakly in the region. Partial FTIR spectra (800–1200 cm<sup>-1</sup>) of (*E*)- and (*Z*)-2-pentene (10 torr) are

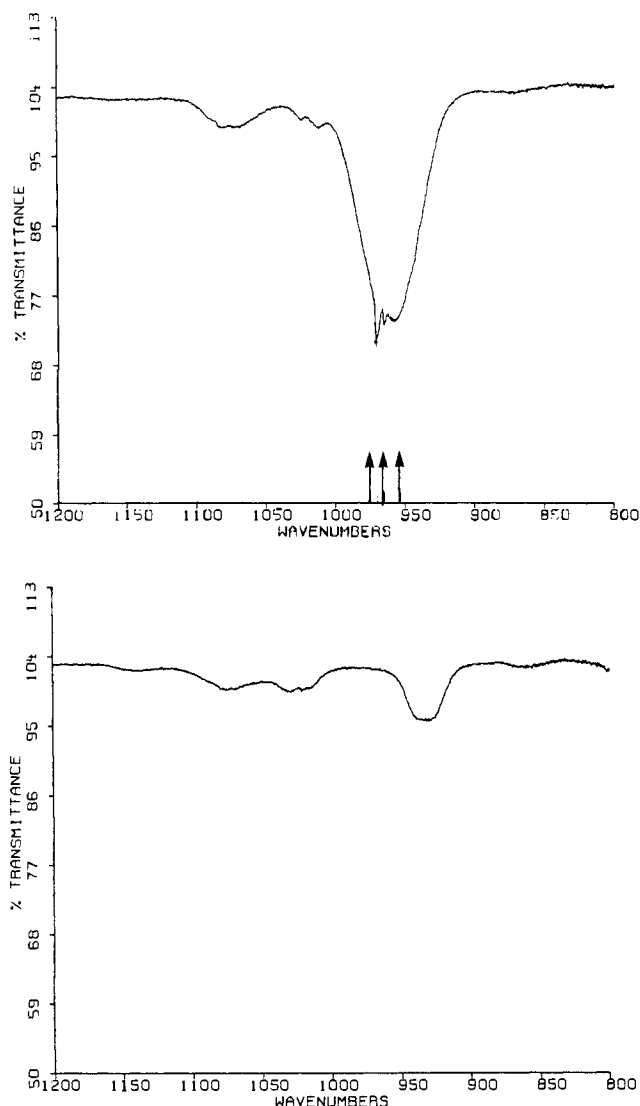
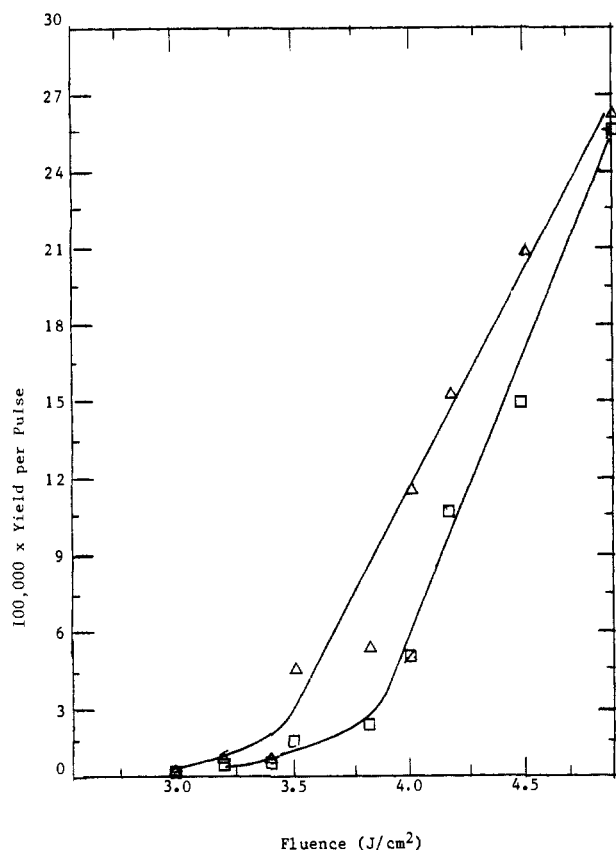


Figure 1. (a, top) FTIR spectrum of (*E*)-2-pentene (10 torr) and (b, bottom) (*Z*)-2-pentene (10 torr) in a 1.0-dm path length cell. Laser excitation frequencies are indicated by vertical arrows on the horizontal axis.

shown in Figure 1. Similar spectra are obtained for the isomeric 2-butenes and 2-hexenes. Single photon absorption cross sections ( $\sigma_{0,1}$ ) for the (*E*)- and (*Z*)-2-alkenes at the frequencies used for IRMP excitation are given in Table I. By definition  $\sigma_{0,1} = \ln(T/T_0)/NL$ , where  $T$  and  $T_0$  are the percent transmittance at some frequency where the sample does not absorb and at a given frequency,  $N$  is the number of molecules per cubic centimeter, and  $L$  is the path length in centimeters. In all cases, the cross section for the *E* isomer is greater than that of the *Z* isomer, allowing selective excitation of the *E* isomer.

Pulsed IRMP excitation of the (*E*)-2-alkenes results in the formation of their *Z* isomers and variable yields of fragmentation products. The laser fluence dependence of the per pulse yields of (*Z*)-2-pentene and fragmentation products (C<sub>1</sub>–C<sub>4</sub> hydrocarbons and pentadienes) from (*E*)-2-pentene is shown in Figure 2. Both reactions have a threshold fluence (ca. 3.0 J/cm<sup>2</sup>) below which products cannot be detected by analytical GC even after repeated pulsing ( $>1000$  pulses). The yields of both isomerization and fragmentation products increase with increasing fluence. Per pulse yields for *E* → *Z* isomerization of the 2-alkenes at several laser frequencies and fluences are summarized in Table I. The observed yields increase with increasing cross section and laser fluence. Isomerization is not observed to occur when  $\sigma_{0,1} < 0.80 \times 10^{-19}$  cm<sup>2</sup> using fluences of 2–5 J/cm<sup>2</sup>. At higher fluences, dielectric breakdown can occur, resulting in extensive fragmentation without appreciable isomerization. Thus we have been unable to study

(9) Bellamy, L. J. *Infrared Spectra of Complex Molecules*; Chapman and Hall: London, 1975; Chapter 3.



**Figure 2.** Fluence dependence of the isomerization ( $\Delta$ ) and fragmentation ( $\square$ ) yields of (*E*)-2-pentene irradiated at  $969\text{ cm}^{-1}$ .

**Table II.** Single and Multiphoton Absorption Cross Sections for Crotonitrile

cross section	$\nu_{\text{exc}}$ , $\text{cm}^{-1}$	$10^{20}\sigma_{E_i}$ , $\text{cm}^2$	$10^{20}\sigma_{Z_i}$ , $\text{cm}^2$	$\sigma_E/\sigma_Z$
$\sigma_{0,1}^a$	931	6.4	0.89	7.2
$\sigma_n^b$	931	5.2	0.84	6.2
$\sigma_{0,1}^a$	978	4.5	0.43	10.5
$\sigma_n^b$	978	3.8	0.56	6.6

<sup>a</sup>Single photon absorption cross sections ( $\pm 10\%$ ). <sup>b</sup>Multiphoton absorption cross sections ( $\pm 20\%$ ).

*Z*  $\rightarrow$  *E* isomerization of the (*Z*)-alkenes using our pulsed  $\text{CO}_2$  laser.

The ratio of isomerization/fragmentation is dependent upon the structure of the 2-alkene and the laser fluence. Excitation of the (*E*)-2-alkenes at  $975\text{ cm}^{-1}$  with a laser fluence of  $3.5\text{ J/cm}^2$  results in isomerization/fragmentation ratios of 3.0 for 2-butene, 1.9 for 2-pentene, and 0.44 for 2-hexene. In addition to *E*  $\rightarrow$  *Z* isomerization, (*E*)-2-butene forms ca. 4% 1-butene and 0.5% 1,3-butadiene upon IRMP excitation under these conditions. No terminal alkene or conjugated diene products were observed from 2-pentene or 2-hexene.

**Reactions of Crotonitrile and Crotonic Esters.** Both (*E*)- and (*Z*)-crotonitrile have moderately intense absorption bands due to  $\text{CH}=\text{CH}$  out-of-plane deformations centered at ca.  $950\text{ cm}^{-1}$  (Figure 3).<sup>10</sup> Rotational fine structure, similar to that reported for acrylonitrile,<sup>10b</sup> is apparent in the spectrum of (*E*)-crotonitrile. Single photon absorption cross sections ( $\sigma_{0,1}$ ) for both isomers at several frequencies are given in Table I. Multiphoton absorption cross sections ( $\sigma_n$ ) have also been determined for (*E*)- and (*Z*)-crotonitrile by both calorimetric measurement of the laser beam intensity and by photoacoustic measurements. Plots of the average number of photons absorbed per pulse,  $\langle N \rangle$ , as

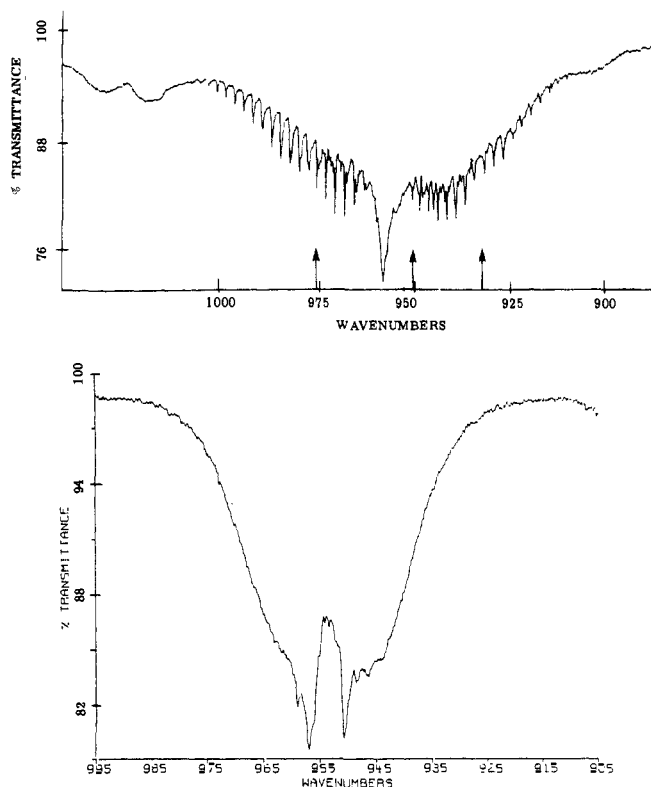


**Figure 3.** (a, top) FTIR spectrum of (*E*)-crotonitrile (7.0 torr) and (b, bottom) (*Z*)-crotonitrile (11.7 torr) in a 1.0-dm path length cell. Laser excitation frequencies are indicated by vertical arrows on the horizontal axis.

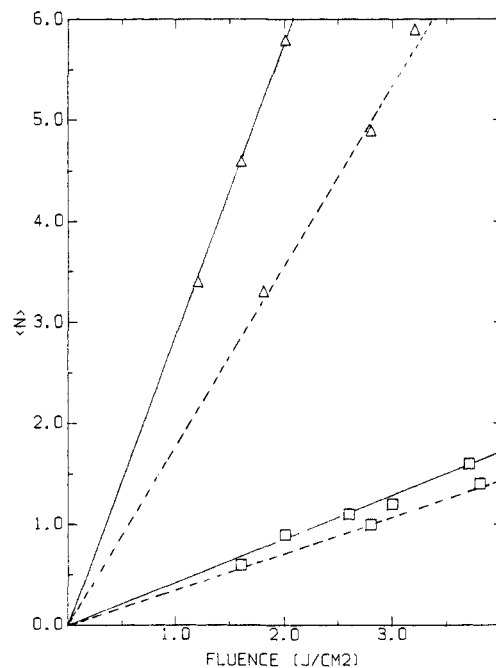


**Figure 4.** Fluence dependence of the average number of photons absorbed per molecule,  $\langle N \rangle$ , by (*E*)-crotonitrile ( $\Delta$ ) and (*Z*)-crotonitrile ( $\square$ ) using  $931\text{-cm}^{-1}$  (—) and  $978\text{-cm}^{-1}$  (---) irradiation.

determined calorimetrically, vs. laser fluence are shown in Figure 4. These plots are linear over the fluence range investigated, thus indicating that  $\sigma_n$  is constant for average excitation levels  $\langle N \rangle \leq 6$  for (*E*)-crotonitrile and  $\langle N \rangle \leq 2$  for (*Z*)-crotonitrile. The value of  $\sigma_n$  equals  $E/N\Phi k$ , where  $E$  is the energy absorbed per torr of absorbing gas,  $N$  is the number of absorbing molecules per torr, and  $\Phi k$  is the laser fluence. Values obtained from the data in Figure 4 are given in Table II along with values of  $\sigma_{0,1}$  obtained from the gas-phase FTIR spectra. The values of  $\sigma_{0,1}$

(10) (a) George, W. O.; Hassid, D. V.; Harris, W. C.; Maddams, W. F. *J. Chem. Soc., Perkin Trans. 2* **1975**, 392. (b) Cowles, J. R.; George, W. O.; Fately, W. G. *J. Chem. Soc., Perkin Trans. 2* **1975**, 396.

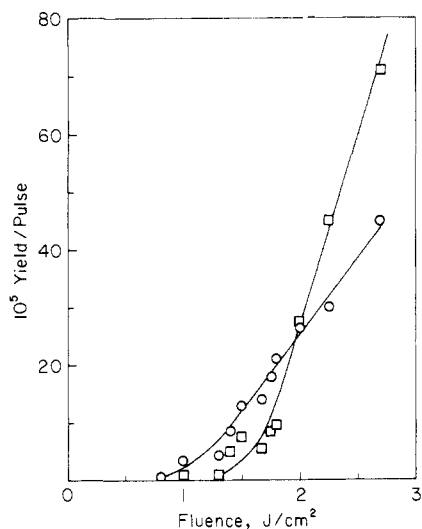


Figure 5. Fluence dependence of the isomerization (O) and fragmentation (□) yields of (*E*)-methyl crotonate irradiated at 975  $\text{cm}^{-1}$ .

and  $\sigma_n$  differ by less than the uncertainty in their measurement ( $\pm 10\%$  and  $\pm 20\%$ , respectively). Photoacoustic measurements of  $\sigma_n$  provide results similar to those obtained calorimetrically.

IRMP irradiation of (*E*)-crotononitrile results in clean  $E \rightarrow Z$  isomerization with a threshold fluence of 2.5  $\text{J}/\text{cm}^2$  ( $\nu_{\text{ex}} = 951 \text{ cm}^{-1}$ ). Fragmentation is not observed for fluences below that necessary for dielectric breakdown (ca. 5  $\text{J}/\text{cm}^2$ ). Per pulse yields for  $E \rightarrow Z$  isomerization at several excitation frequencies and fluences are given in Table I. As in the case of the 2-alkenes, per pulse yields increase with increasing fluence and cross section. Irradiation of (*Z*)-crotononitrile at 951  $\text{cm}^{-1}$  results in formation of the *E* isomer; however, maximum conversions are  $< 5\%$ . Irradiation of a mixture of (*E*)-crotononitrile and the transparent thermal monitor<sup>7c</sup> ethyl acetate (0.1 torr) at 931  $\text{cm}^{-1}$  results in isomerization of crotononitrile without fragmentation of ethyl acetate.

Irradiation of (*E*)-methyl crotonate at 975  $\text{cm}^{-1}$  results in both isomerization and fragmentation to  $\text{CO}_2$  and  $\text{C}_1\text{--C}_4$  hydrocarbons. The fluence dependence of the per pulse yields is shown in Figure 5. The threshold fluence for observation of product formation is ca. 0.75  $\text{J}/\text{cm}^2$ , substantially lower than the values for the 2-alkenes or crotononitrile. The low threshold and observation of dielectric breakdown at fluences greater than 3  $\text{J}/\text{cm}^2$  are consequences of the very large single photon absorption cross section for methyl crotonate.<sup>10a</sup> The ratio of isomerization/fragmentation products decreases with increasing laser fluence from a value of 3.5 at 1.0  $\text{J}/\text{cm}^2$  to 0.63 at 2.7  $\text{J}/\text{cm}^2$ . Irradiation of (*E*)-ethyl crotonate at 975  $\text{cm}^{-1}$  yields ca. 99% crotonic acid and ethylene and  $\leq 1\%$  (*Z*)-ethyl crotonate over the entire fluence range 0.9–3.0  $\text{J}/\text{cm}^2$ .

**Irradiation of 1,3- and 1,4-Pentadienes.** Infrared spectra of (*E*)- and (*Z*)-1,3-pentadiene and 1,4-pentadiene are shown in Figure 6. All three isomers have two moderately intense absorption bands between 850 and 1050  $\text{cm}^{-1}$ .<sup>11</sup> Single photon absorption cross sections for (*E*)- and (*Z*)-1,3-pentadiene at several laser frequencies are given in Table III. The ratio of cross sections for the two isomers,  $\sigma_E/\sigma_Z$ , varies from 1.1 at 931  $\text{cm}^{-1}$  to 1.6 at 982  $\text{cm}^{-1}$ .

Irradiation of either (*E*)- or (*Z*)-1,3-pentadiene at 931 or 953  $\text{cm}^{-1}$  with fluences less than 3  $\text{J}/\text{cm}^2$  results in the formation of the same mixture of *E* and *Z* isomers without competing fragmentation or isomerization reactions. This mixture of isomers is dependent upon excitation frequencies but is independent of laser fluence (2.7–3.1  $\text{J}/\text{cm}^2$  at 953  $\text{cm}^{-1}$ ). Continued irradiation does not alter the isomer ratios given in Table III. In contrast, irradiation at 982  $\text{cm}^{-1}$  with ca. 400 pulses (2.2  $\text{J}/\text{cm}^2$ ) effects

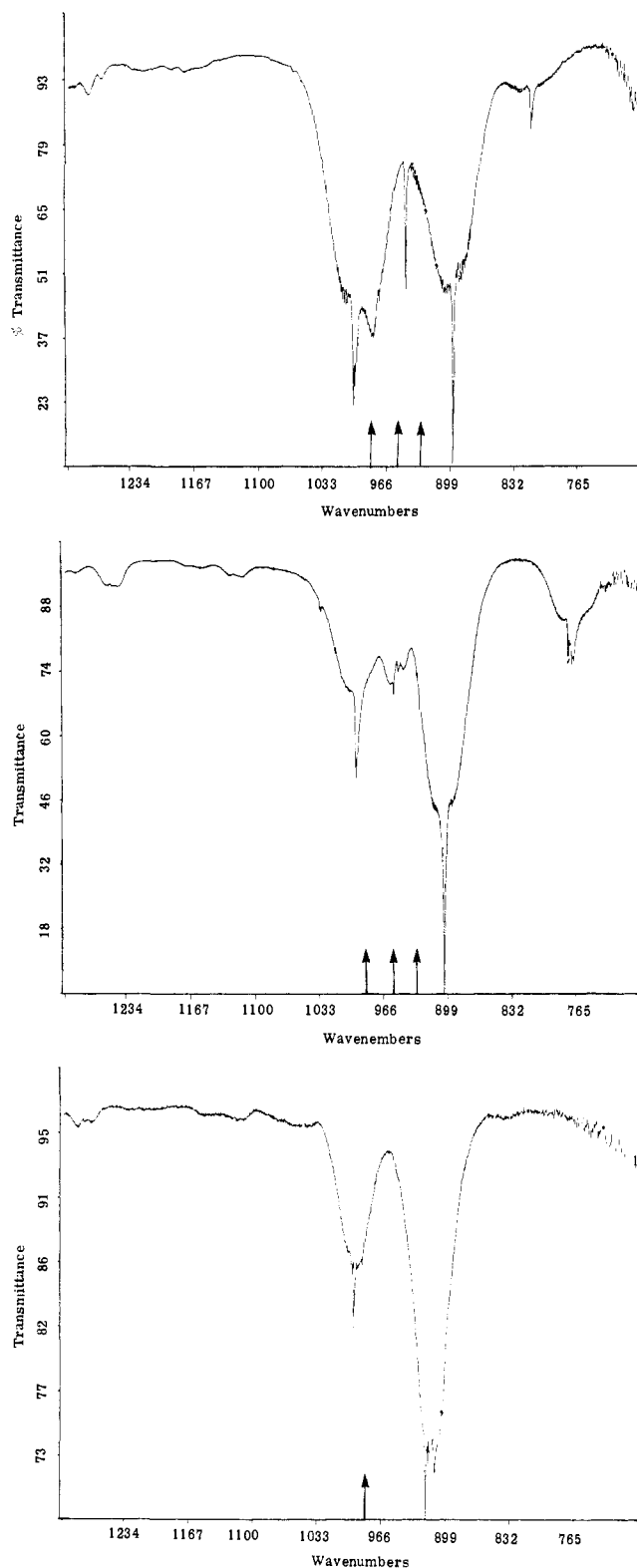


Figure 6. FTIR spectrum of (a, top) (*E*)-1,3-pentadiene (20 torr), (b, middle) (*Z*)-1,3-pentadiene (20 torr), and (c, bottom) 1,4-pentadiene (20 torr) in a 1.0-dm path length cell. Laser excitation frequencies are indicated by vertical arrows on the horizontal axis.

$E \rightarrow Z$  isomerization but not  $Z \rightarrow E$  isomerization, resulting in  $> 90\%$  conversion of (*E*)- to (*Z*)-1,3-pentadiene (Figure 7). Per pulse yields for  $E \rightarrow Z$  isomerization determined at  $< 5\%$  conversion of the parent isomer are summarized in Table III. Yields are seen to increase with increasing laser fluence for 953- $\text{cm}^{-1}$  excitation.

Irradiation of (*E*)- or (*Z*)-1,3-pentadiene with fluences greater than 3  $\text{J}/\text{cm}^2$  at 982  $\text{cm}^{-1}$  results in the formation of cyclopentadiene and trace amounts of 1,4-pentadiene. For example,

(11) Compton, D. A. C.; George, W. O.; Maddams, W. F. *J. Chem. Soc., Perkin Trans. 2* 1977, 1311.

Table III. Frequency and Fluence Dependence of per Pulse Yields and Stationary States for 1,3-Pentadiene

$\nu_{\text{C-X}}$ , cm <sup>-1</sup>	$10^{19}\sigma_E$ , cm <sup>2</sup>	$10^{19}\sigma_Z$ , cm <sup>2</sup> <sup>a</sup>	$\sigma E/\sigma Z$	fluence, J/cm <sup>2</sup>	(10 <sup>5</sup> yield/pulse) <sup>b</sup>		steady-state <sup>c</sup> % Z
					E → Z	Z → E	
931	2.7	2.4	1.1	2.7	310	210	60 (63)
953	2.4	2.1	1.2	2.7	41	12	77 (80)
				2.9	145	44	77 (80)
				3.1	310	89	78 (80)
				2.7	300	<0.1	(>95)
982	3.2	2.1	1.6	2.7	300	<0.1	(>95)

<sup>a</sup>Single photon absorption cross section obtained from infrared absorption spectrum ( $\pm 10\%$ ). <sup>b</sup>Yield of molecules in irradiated volume converted to per pulse yields at low conversions ( $< 5\%$ ). <sup>c</sup>Values calculated from single pulse yields or the observed stationary state (values in parentheses).

Table IV. Kinetic and Thermodynamic Data for Unimolecular Reactions

reaction	log <i>A</i>	<i>E</i> <sub>a</sub> , kcal/mol	ref	$\Delta H$ , kcal/mol	$\Delta S$ , cal/(mol K)	ref
(Z)-2-butene → (E)-2-butene	13.8	63	12a	-1.04	-1.22	12f
(Z)-2-butene → 1-butene	13.5	72	12a			
(E)-2-butene → 1,3-butadiene + H <sub>2</sub>	13	65	12a			
(Z)- or (E)-2-butene → C <sub>3</sub> H <sub>5</sub> + CH <sub>3</sub>	16	98	12g			
(Z)-2-pentene → (E)-2-pentene	14	63	12d	-1.17	-0.85	12f
(Z)- or (E)-2-pentene → C <sub>4</sub> H <sub>7</sub> + CH <sub>3</sub>	16	76	12b			
(Z)-2-hexene → (E)-2-hexene	14	63	12d	-0.82	0.01	12e <sup>d</sup>
(Z)- or (E)-2-hexene → C <sub>4</sub> H <sub>7</sub> + C <sub>2</sub> H <sub>5</sub>	16	72	12g			
(Z)-crotonitrile → (E)-crotonitrile	13.2	58	13b	+0.17	-0.39	13a
(Z)-methyl crotonate → (E)-methyl crotonate	13.2	58	14a	-0.2	2.7	14a
(Z)-methyl crotonate → methyl vinylacetate	9.0	43	14a			
ethyl acetate → acetic acid + C <sub>2</sub> H <sub>4</sub>	12.6	48	7c			
(Z)-1,3-pentadiene → (E)-1,3-pentadiene	13.6	53	13b	-1.04	-0.14	15a
(E)-1,3-pentadiene → cyclopentadiene + H <sub>2</sub>	13	65	15b			
1,4-pentadiene → 1,3-pentadiene		≤75	12g			

<sup>d</sup>Data for 2-heptene.

irradiation of (E)-1,3-pentadiene with 150 pulses of 3.5 J/cm<sup>2</sup> fluence results in the formation of a mixture consisting of (E)-1,3-pentadiene (5.4%), (Z)-1,3-pentadiene (35.6%), cyclopentadiene (34.4%), cyclopentene (0.5%), and 1,4-pentadiene (0.2%). Products were characterized by comparison of their GC retention times and mass spectral fragmentation with authentic samples, and cyclopentadiene was further characterized by GC/FTIR. The threshold for the formation of cyclopentadiene is higher than that for E → Z isomerization but lower than the threshold for C-C bond fragmentation reactions.

Irradiation of 1,4-pentadiene with a fluence of 3.4 J/cm<sup>2</sup> at 982 cm<sup>-1</sup> results in the formation of (E)- and (Z)-1,3-pentadienes and cyclopentadiene in a ratio of ca. 1:1:4. Increasing the fluence to 3.7 J/cm<sup>2</sup> increases the yield/pulse for all isomers and gives a product ratio of 1:4:10. The yield of 1,3-pentadienes and cyclopentadiene as a function of argon buffer gas pressure after 250 laser pulses of 3.3 J/cm<sup>2</sup> fluence at 942 cm<sup>-1</sup> is shown in Figure 8. The yields of both products are reduced by added argon, and the ratio of cyclopentadiene/1,3-pentadiene decreases from 1.6 at 0 torr of argon to 0.3 at 1.5 torr of argon.

## Discussion

The thermal unimolecular isomerization and fragmentation reactions of 2-alkenes,<sup>12</sup>  $\alpha,\beta$ -unsaturated nitriles<sup>13</sup> and esters,<sup>14</sup> and 1,3-pentadienes<sup>15</sup> have previously been investigated by using conventional methods of thermal activation. Kinetic and thermodynamic parameters for Z → E isomerization reactions and other selected unimolecular reactions of these molecules are summarized in Table IV. In all cases except that of crotonitrile, the E isomer is thermodynamically more stable than the Z isomer

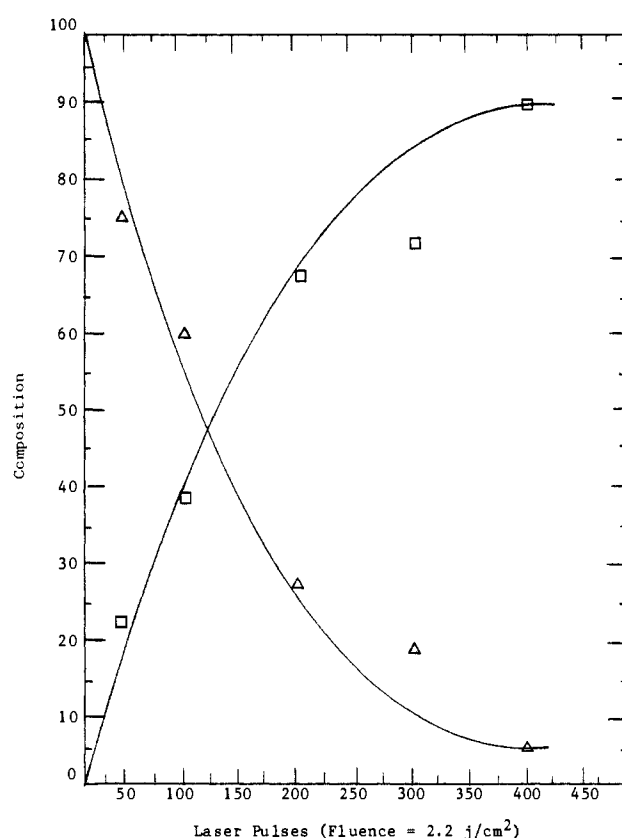


Figure 7. IRMP isomerization of (E)-1,3-pentadiene ( $\Delta$ ) to (Z)-1,3-pentadiene ( $\square$ ) using 982-cm<sup>-1</sup> irradiation and a laser fluence of 2.2 J/cm<sup>2</sup>.

at room temperature. The three 2-alkenes and 1,3-pentadienes have values of  $\Delta H \sim -1$  kcal/mol and small negative values of  $\Delta S$  for Z → E isomerization. Values of log *A* for Z → E isomerization are all  $13.5 \pm 0.3$ , while values of *E*<sub>a</sub> decrease from ca. 63 kcal/mol for the 2-alkenes to 58 kcal/mol for crotonitrile and methyl crotonate and 53 kcal/mol for 1,3-pentadiene.

(12) (a) Alfassi, Z. B.; Golden, D. M.; Benson, S. W. *Int. J. Chem. Kinet.* **1973**, *5*, 991. (b) Jeffers, P.; Bauer, S. H. *Int. J. Chem. Kinet.* **1974**, *6*, 763. (c) Masson, D.; Richard, C.; Martin, R. *Int. J. Chem. Kinet.* **1976**, *8*, 37. (d) Bauer, S. H.; Yavada, B. P.; Jeffers, P. *J. Phys. Chem.* **1974**, *78*, 770. (e) Egger, K. W. *J. Am. Chem. Soc.* **1967**, *89*, 504. (f) Kapteijn, F.; van der Steen, A. J.; Mol, J. C. *J. Chem. Thermodyn.* **1983**, *15*, 137. (g) Egger, K. W.; Cocks, A. T. *Helv. Chem. Acta* **1973**, *56*, 1517.

(13) (a) Butler, J. N.; McAlpine, R. D. *Can. J. Chem.* **1963**, *41*, 2487. (b) Marley, W. M.; Jeffers, P. M. *J. Phys. Chem.* **1975**, *79*, 2085.

(14) Butler, J. N.; Small, G. J. *Can. J. Chem.* **1963**, *41*, 2492.

(15) (a) Egger, K. W.; Benson, S. W. *J. Am. Chem. Soc.* **1965**, *87*, 3311. (b) Nguyen, T. T.; King, K. D. *Int. J. Chem. Kinet.* **1982**, *14*, 623.

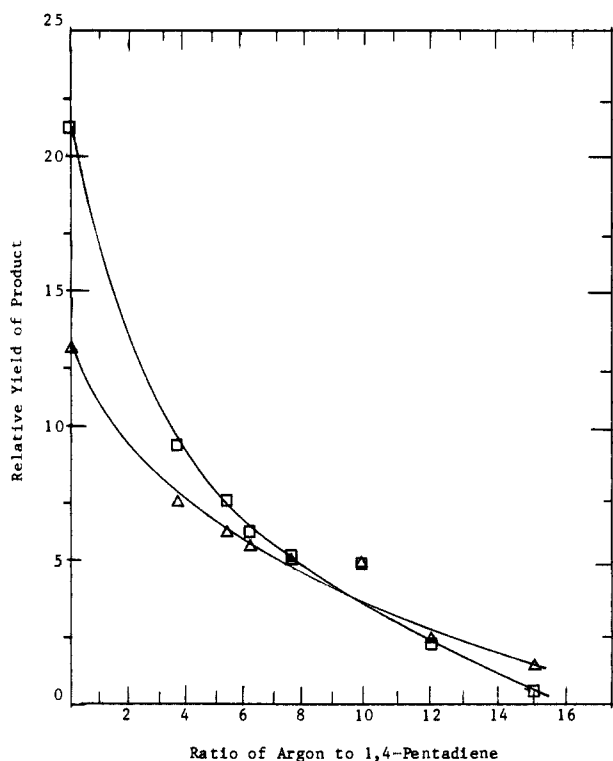


Figure 8. Argon buffer gas dependence of the yields of cyclopentadiene ( $\square$ ) and 1,3-pentadiene ( $\Delta$ ) from 1,4-pentadiene using 250 pulses of  $942\text{-cm}^{-1}$  irradiation with a fluence of  $3.3\text{ J/cm}^2$ .

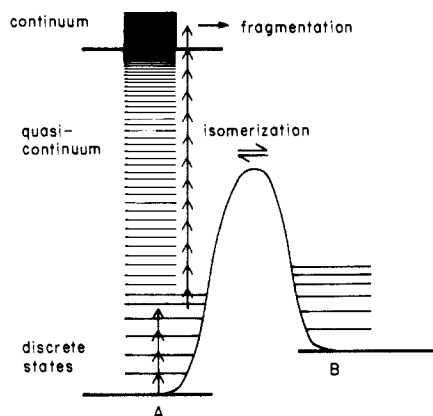


Figure 9. Model schematic representation of the multiphoton excitation, contrathermodynamic isomerization, and fragmentation processes.

Conjugation can lower  $E_a$  for  $Z \rightarrow E$  isomerization either by stabilizing the twisted 1,2-biradical or dipolar transition state more than the ground state<sup>16</sup> or by providing an alternative isomerization mechanism, viz., conrotatory cyclization to and ring opening of a cyclobutene intermediate.<sup>17</sup>

IRMP excitation of alkenes differs from normal collisional activation in that energy is introduced into molecular vibrations and only those molecules which absorb at the laser frequency are initially excited. A schematic model for multiphoton excitation resulting in contrathermodynamic isomerization and fragmentation is shown in Figure 9. Details of this model have recently been discussed.<sup>1b</sup> In order for contrathermodynamic isomerization to occur, several conditions must be fulfilled: (a) the more stable isomer must absorb infrared radiation more strongly than the less stable isomer at a  $\text{CO}_2$  laser frequency; (b) the more stable isomer (but not the less stable isomer) must absorb sufficient infrared quanta within a laser pulse to produce a finite population of

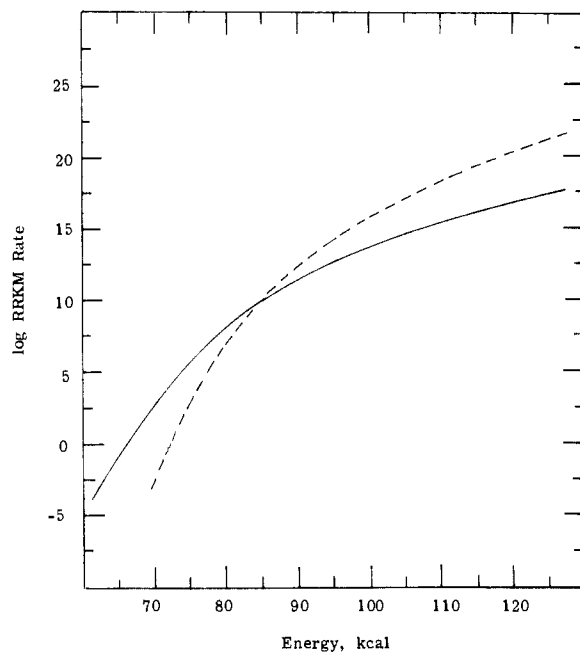


Figure 10. Calculated RRKM rates for isomerization (—) and fragmentation (---) of (*E*)-2-pentene vs. reactant energy.

molecules with sufficient energy to undergo reversible isomerization but not fragmentation; and (c) collisional deactivation of vibrationally excited reactant and product molecules must occur between laser pulses and provide a finite yield of product from each laser pulse.

As seen in Figures 1, 3, and 6, (*E*)-alkenes and -dienes absorb more strongly than their *Z* isomers at wavelengths accessible with a  $\text{CO}_2$  laser. Due to the threshold nature of the IRMP isomerization process, small differences in absorption cross sections are sufficient to allow highly selective isomerization (vide infra). We have previously demonstrated that conditions (b) and (c) above can be fulfilled by using a collimated laser beam of uniform intensity and moderate pulse duration with sufficiently low gas pressure ( $<0.5$  torr) to ensure that a significant number of collisions do not occur in the irradiated portion of the cell during the laser pulse.<sup>3</sup> The absence of collisional redistribution of vibrational energy was confirmed in the case of (*E*)-crotonitrile by irradiation in the presence of ethyl acetate, a transparent thermal monitor<sup>7c</sup> with a lower  $E_a$  for decomposition than that for crotonitrile isomerization (Table IV).

We have also confirmed, in the case of (*E*)- and (*Z*)-crotonitrile, that the absorption cross section does not change with increasing laser fluence (Figure 4). Such behavior is characteristic of large organic molecules for which excitation from the region of discrete states into the quasi-continuum occurs without the "bottleneck" behavior observed for small molecules.<sup>5</sup> As discussed previously,<sup>3b</sup> the energy corresponding to the mean number of absorbed photons does not necessarily correlate with the mean energy of a reacting molecule since reaction normally takes place in the high energy tail of the distribution of IRMP excited molecules.

**Reactions of 2-Alkenes.** Early attempts to effect  $E \rightarrow Z$  isomerization of (*E*)-2-butene by IRMP excitation resulted in extensive fragmentation to  $\text{C}_1\text{-C}_3$  hydrocarbons and low yields of (*Z*)-2-butene.<sup>18</sup> The use of better controlled excitation conditions ( $975\text{-cm}^{-1}$  irradiation, fluence  $\sim 3.5\text{ J/cm}^2$ ) allows quantitative conversion of (*E*)-2-butene to a mixture of 75% (*Z*)-2-butene and small amounts of 1-butene, 1,3-butadiene, and other fragmentation products. Increasing the laser fluence increases the yield/pulse for both isomerization and fragmentation products, as shown in Figure 2 for (*E*)-2-pentene. Both isomerization and fragmentation have reaction thresholds between 3.0

(16) Benson, S. W. *Thermochemical Kinetics*; Wiley: New York, 1968; p 72.

(17) Stephenson, L. M.; Gemmer, R. V.; Brauman, J. I. *J. Am. Chem. Soc.* **1972**, *94*, 8620.

(18) Yogev, A.; Lowenstein-Benmair, R. M. *J. Am. Chem. Soc.* **1973**, *95*, 8487.

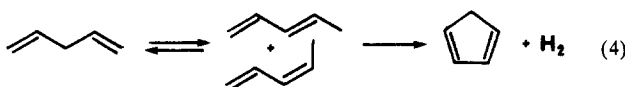


and cross sections for stimulated emission) must be considered in describing the steady state for IRMP-induced reversible isomerization reactions, the significant conclusion that can be drawn from the results in Tables I and III is that *only modest differences in absorption cross sections are sufficient to allow highly selective contrathermodynamic isomerization of the more strongly absorbing isomer.*

IRMP excitation of (*E*)- or (*Z*)-1,3-pentadiene at 931  $\text{cm}^{-1}$  with a fluence greater than 3  $\text{J}/\text{cm}^2$  results in >90% conversion to cyclopentadiene and trace amounts of 1,4-pentadiene and cyclopentene. Nonselective fragmentation of the pentadienes is observed using fluences greater than 5  $\text{J}/\text{cm}^2$ . Loss of  $\text{H}_2$  from (*Z*)-1,3-pentadiene has been observed by Nguyen and King<sup>15b</sup> to occur with the activation parameters reported in Table IV. They assigned the product as 1,2,4-pentatriene on the basis of a  $m/e$  66 peak in the mass spectrum. We have assigned the product of the IRMP-induced reaction as cyclopentadiene on the basis of its spectroscopic properties. While the mechanism of unimolecular loss of  $\text{H}_2$  to yield cyclopentadiene remains to be elucidated, its occurrence at a threshold fluence higher than that for  $Z \rightarrow E$  isomerization but lower than that for fragmentation is consistent with the reported activation parameters.<sup>15b</sup>

The observation of trace amounts of 1,4-pentadiene upon IRMP excitation of (*E*)- or (*Z*)-1,3-pentadiene indicates that positional isomerization occurs by a unimolecular reaction pathway, as is the case for the 2-butenes. Since the isomerization of 1,3- to 1,4-pentadiene is substantially endothermic (ca. 7 kcal/mol), it is not surprising that 1,4-pentadiene was not detected as a product of low-pressure pyrolysis of 1,3-pentadiene.<sup>15b</sup> In order to obtain further information about the positional isomerization reaction, the IRMP-induced reactions of 1,4-pentadiene were investigated.

IRMP irradiation of 1,4-pentadiene at 942  $\text{cm}^{-1}$  to  $\leq 10\%$  conversion results in the formation of (*E*)- and (*Z*)-1,3-pentadiene and cyclopentadiene. Prolonged irradiation results in essentially quantitative conversion to cyclopentadiene, as is observed for irradiation of the 1,3-pentadienes under these conditions. The ratio of (*Z*/*E*)-1,3-pentadienes increases with increasing laser fluence. This increase is consistent with initial isomerization of 1,4-pentadiene to yield (*E*)-1,3-pentadiene followed by selective  $E \rightarrow Z$  isomerization. The ratio of cyclopentadienes to 1,3-pentadienes also increases with increasing laser fluence. Higher laser fluence is known to enhance the yield of secondary products in consecutive IRMP-induced reactions.<sup>1b</sup> Thus, the increase in the cyclopentadiene/1,3-pentadiene ratio with increasing laser fluence may be indicative of a consecutive reaction mechanism in which positional isomerization precedes loss of  $\text{H}_2$  (eq 4).



Support for such a mechanism is provided by the observed effect of added argon buffer gas on the relative yields of cyclopentadiene and 1,3-pentadienes formed from 1,4-pentadiene (Figure 8). Collisions of the vibrationally excited reactant (1,4-pentadiene) with argon should lower its average energy content and hence the yields of all products, while collisions of the primary product (1,3-pentadiene) with argon should increase its yield relative to that of the secondary product (cyclopentadiene). This is consistent with the observed decrease in the cyclopentadiene/1,3-pentadiene ratio with increasing Ar pressure.

The above results indicate that (*E*)- and (*Z*)-1,3-pentadienes are the predominant primary products of IRMP excitation of 1,4-pentadiene at fluences below the threshold for fragmentation. As in the case for isomerization of (*E*)-2-butene to 1-butene, the use of low reaction pressure and a "wall-free" reactor make a free-radical mechanism for positional isomerization seem highly unlikely. As such, an upper limit for the activation energy of the 1,3-hydrogen shift or sequential 1,2-hydrogen shift is provided by the 75 kcal/mol C-H bond dissociation energy of 1,4-pentadiene.<sup>20</sup> This value is low enough to permit selective IRMP isomerization vs. fragmentation and is higher than the activation energy for loss of  $\text{H}_2$  from 1,3-pentadiene (Table IV). Thus

conventional thermolysis of 1,4-pentadiene should yield only the secondary product, cyclopentadiene, and not the kinetically labile primary product, 1,3-pentadiene. To our knowledge, the uncatalyzed unimolecular reactions of 1,4-pentadiene have not previously been investigated.

### Concluding Remarks

Our investigation of the IRMP laser-induced reactions of alkenes and dienes has established that it is possible to achieve essentially quantitative  $E \rightarrow Z$  isomerization of alkenes and dienes even in cases where the *Z* isomer is thermodynamically less stable than the *E* isomer at room temperature. Only modest differences in the infrared absorption cross sections are necessary for the observation of highly selective isomerization due to the amplification of cross-sectional differences in the multiphoton excitation process.

The principal limitations on IRMP contrathermodynamic isomerization reactions are imposed by competing fragmentation reactions and by the inhomogeneity and energy fluctuations in the infrared laser pulse. Isomerization/fragmentation ratios are observed to increase as the  $E_a$  for isomerization decreases (2-alkenes < crotononitrile or 1,3-pentadiene) or as  $E_a$  for fragmentation increases (2-hexene < 2-pentene < 1-butene). Since fragmentation reactions have higher preexponential factors than isomerization reactions, isomerization/fragmentation ratios also increase with decreasing laser fluence, thus allowing a limited degree of control over the product ratios for competing reactions by simply varying the laser fluence.

In addition to  $E \rightarrow Z$  isomerization, we have observed positional isomerization as minor reaction pathways for IRMP excitation of 2-butene and 1,3-pentadiene, yielding 1-butene and 1,4-pentadiene, respectively, and as the major isomerization pathway for 1,4-pentadiene, yielding 1,3-pentadiene. In addition to fragmentation via C-C cleavage, loss of  $\text{H}_2$  is a minor reaction pathway for (*E*)-2-butene and 1,3-pentadiene leading to 1,3-butadiene and cyclopentadiene, respectively. Further investigation of the positional isomerization and cyclopentadiene formation using deuterated pentadienes might provide the information necessary to distinguish between concerted vs. multistep mechanisms for these unusual unimolecular reactions.

### Experimental Section

**Chemicals.** Ethylene (Matheson), (*E*)- and (*Z*)-2-butenes (Phillips pure grade), (*E*)- and (*Z*)-2-pentenenes (Chemical Samples), (*E*)-2-hexene (Aldrich), (*Z*)-2-hexene (Fluka), (*Z*)-1,3-pentadiene (Fluka), (*E*)-1,3-pentadiene (Aldrich), (*E*)-1,4-pentadiene (Aldrich), and 1,3-cyclohexadiene (Aldrich) were found to be >99% pure by gas chromatographic (GC) analysis and were used as received without further purification. Cyclopentadiene dimer (Aldrich) was distilled to obtain cyclopentadiene, and methyl and ethyl crotonates (Aldrich) were distilled prior to use. (*E*)- and (*Z*)-crotononitriles (Aldrich) were obtained as a mixture of isomers that was separated by preparative GC using a 10 ft  $\times$  1/4 in. column of 5% FFAP on Chromosorb G.

**Infrared Irradiation.** Infrared irradiation of various alkenes was performed by using the output of a Lumonics K203-2 TEA laser. Output pulses were monitored with a photon drag detector and consisted of a sharp (60 ns) spike containing ca. 70% of the pulse energy followed by a low intensity tail of approximately 0.5- $\mu\text{s}$  duration. The laser was triggered at a rate of 0.5 Hz and produced a nonuniform output beam that was spatially filtered with an iris for accurate definition of the beam area. The beam profile was monitored periodically via burn patterns on heat-sensitive paper. Variation of fluence was achieved by collimation of the beam with a Galilean telescope and laser energies were measured with a Scientech calorimeter. Laser lines were determined with an Optical Engineering  $\text{CO}_2$  laser spectrum analyzer. The laser was contained in a shielded room to eliminate electrical noise.

Samples were contained in 1.0-dm path length Pyrex cells of 2.5 cm i.d. with NaCl entrance and exit windows fitted to the cell with Viton O-rings. High-vacuum Kontes valves were used to connect the cells to a vacuum line for sample preparation or to a GC, GC/MS, or GC/FTIR for product analysis. A sample pressure of 0.1 torr was used in all cases. Cell pressures were measured with a MKS capacitance monometer.

**Absorption Cross-Sectional Measurements.** Transmittance values were obtained from gas-phase FTIR spectra recorded on a Nicolet Series 7000 FTIR. Samples (5–20 torr) were contained in a 1.0-dm path length Pyrex cell fitted with NaCl windows. Spectra of the sample and blank



cell were ratioed to produce a percent transmittance spectrum. A resolution of 0.5 wavenumbers was obtained.

The single photon absorption cross section at a given frequency is defined as  $\sigma_{0,1} = \ln(T/T_0)/(NL)$ , where  $T$  is the percent transmittance at some frequency the sample does not absorb and  $T_0$  is % transmittance at a given frequency.  $N$  is the number density (number of molecules per cubic centimeter at a given pressure and temperature) and  $L$  is the path length of the cell in centimeters. The resulting units of  $\sigma_{0,1}$  are centimeters squared.

Multiphoton absorption cross sections were determined both by calorimetric and photoacoustic methods for (*E*)- and (*Z*)-crotonitriles (0.01–0.25 torr). Calorimetric determination of absorbed energy employed a Scientech calorimeter placed at the exit window of a 43-cm path length Pyrex cell fitted with NaCl windows. Measurements of attenuation of transmitted laser beam intensity were performed over a fluence range of 1–5 J/cm<sup>2</sup>. Photoacoustic determination of absorbed energy was made with an electret microphone (Knowles Electronics, Inc., Model BT-1759) positioned at the center of a 23-cm path length brass photoacoustic cell fitted with BaF<sub>2</sub> windows. Background signals due to window heating were isolated from the volume observed by the microphone by cylindrical constrictions placed at either end of the cell 5 cm from the windows. Signals were fed directly into an oscilloscope. The peak-to-trough amplitude of the first acoustic wave following the laser pulse was measured.

The multiphoton absorption cross section at a given frequency is defined as  $\sigma_n = E/(N\Phi)$ , where  $E$  is the energy absorbed per torr of gas

molecules (J/torr) in the cell volume.  $N'$  is the number of molecules per torr in the cell volume at a given temperature and  $\Phi$  is the laser fluence (J/cm<sup>2</sup>). The average number of photons absorbed  $\langle N \rangle$  are calculated from  $E$ . The resulting units of  $\sigma_n$  are centimeters squared.

**Product Analysis.** Irradiated samples were analyzed by transferring the entire contents of the irradiation cell to a Varian 3700 FID gas chromatograph equipped with a gas sampling valve, interfaced to a Hewlett-Packard 3380 reporting integrator. The GC was operated at room temperature with all columns except for FFAP, which was heated to 80 °C. Products were characterized by GC/mass spectrometry with comparisons made to authentic samples of isomers and selected fragmentation products using a Hewlett-Packard 5985 mass spectrometer. Mass balances of >90% were obtained for all reported data.

(*E*)- and (*Z*)-1,3-pentadienes, -1,4-pentadienes, and -cyclopentadienes were analyzed by using a 12 ft × 19 in. column of 20% dimethylsulfolane on Chromosorb P. (*E*)- and (*Z*)-2-butenes were analyzed by using a 20 ft × 1/8 in. column of 20% propylene carbonate on Chromosorb P. (*E*)- and (*Z*)-2-pentenes and *cis*-2-hexene were analyzed by using a 20 ft × 1/8 in. column of 20% 3,3'-oxydipropionitrile on Chromosorb P. Methyl and ethyl crotonates and (*E*)- and (*Z*)-crotonitriles were analyzed by using a 10 ft × 1/8 in. 5% FFAP column on Chromosorb G.

**Acknowledgment.** We thank the National Science Foundation for support of this work under Grants CHE82-06976 (E. W.) and CHE80-26020 (F.D.L.). The CO<sub>2</sub> laser was purchased with funds provided by National Science Foundation Grant CHE80-09060.

## A New Iodate Oscillator: The Landolt Reaction with Ferrocyanide in a CSTR<sup>1</sup>

Elizabeth C. Edblom,<sup>†</sup> Miklós Orbán,<sup>‡</sup> and Irving R. Epstein\*<sup>†</sup>

Contribution from the Department of Chemistry, Brandeis University, Waltham, Massachusetts 02254, and Institute of Inorganic and Analytical Chemistry, L. Eötvös University, H-1443 Budapest, Hungary. Received November 8, 1985

**Abstract:** At a temperature of 30 °C or higher, the reaction of sulfite, iodate, and ferrocyanide exhibits sustained oscillation in a CSTR. The system may be thought of as a Fe(CN)<sub>6</sub><sup>4-</sup> perturbation of the bistable Landolt (SO<sub>3</sub><sup>2-</sup>–IO<sub>3</sub><sup>-</sup>) reaction in which the ferrocyanide serves to consume the I<sub>2</sub> produced in the reduction of iodate, thereby "resetting the clock". The reaction may be monitored with pH, redox or iodide-selective electrodes, or spectrophotometric measurement of iodine, ferrocyanide, or ferricyanide.

Iodate-based reactions were the first chemical oscillators to be discovered, yet this group has remained much smaller in number than either the bromate- or chlorite-based oscillators.<sup>2</sup> Iodate oscillators characterized to date include the Bray (hydrogen peroxide–iodate) reaction,<sup>3</sup> the Briggs–Rauscher (hydrogen peroxide–manganous–malonic acid–iodate) system,<sup>4</sup> and their variants.<sup>5,6</sup> In addition, a number of systems containing chlorite, iodate, and a reductant exhibit oscillation, though these have been classified as chlorite oscillators.<sup>7</sup> Oscillations have been reported<sup>8</sup> in the arsenite–iodate reaction, but these claims have been challenged,<sup>9</sup> and our own experiments confirm that the system is bistable, i.e., it exhibits two different stable stationary states under the same set of experimental conditions, but it is not oscillatory. Beck et al.<sup>10</sup> have reported "oligo-oscillations" in systems consisting of iodate, sulfite, and various reducing agents.

Many of the recently discovered oscillators have been found with use of a systematic search procedure<sup>11</sup> based upon the cross-shaped phase diagram model of Boissonade and De Kepper.<sup>12</sup> In this approach, one begins with an autocatalytic reaction and adds to it an appropriate feedback species in a continuous flow stirred tank reactor (CSTR). The Landolt-type reactions,<sup>13</sup> which

are autocatalytic oxidations of suitable substrates by iodate, constitute a promising starting point from which to design new iodate-based oscillators. We report here the discovery of a new

(1) Paper 36 in the series *Systematic Design of Chemical Oscillators*. Paper 35: Valdes-Aguilera, O.; Kustin, K.; Epstein, I. R. *J. Phys. Chem.*, submitted for publication.

(2) Epstein, I. R.; Orbán, M. In *Oscillations and Traveling Waves in Chemical Systems*; Field, R. J.; Burger, M., Eds.; Wiley: New York, 1985; p 257.

(3) Bray, W. C. *J. Am. Chem. Soc.* **1921**, *43*, 1262.

(4) Briggs, T. S.; Rauscher, W. C. *J. Chem. Educ.* **1973**, *50*, 496.

(5) Cooke, D. O. *React. Kinet. Catal. Lett.* **1976**, *4*, 329.

(6) Chopin-Dumas, J.; Papel, M. N. In *Non-Equilibrium Dynamics in Chemical Systems*; Vidal, C.; Pacault, A., Eds.; Springer-Verlag: Berlin, 1984; p 69.

(7) Orbán, M.; Dateo, C.; De Kepper, P.; Epstein, I. R. *J. Am. Chem. Soc.* **1982**, *104*, 5911.

(8) Rastogi, R. P.; Das, I.; Singh, A. R. *J. Phys. Chem.* **1984**, *88*, 5132.

(9) Ganapathisubramanian, N.; Showalter, K. *J. Phys. Chem.* **1985**, *89*, 2118.

(10) Rábai, Gy.; Bazsa, Gy.; Beck, M. T. *J. Am. Chem. Soc.* **1979**, *101*, 6746.

(11) Epstein, I. R.; Kustin, K.; De Kepper, P.; Orbán, M. *Sci. Am.* **1983**, *248* (3), 112.

(12) Boissonade, J.; De Kepper, P. *J. Phys. Chem.* **1980**, *84*, 501.

(13) Landolt, H. *Ber. Dtsch. Chem. Ges.* **1886**, *19*, 1317.

<sup>†</sup> Brandeis University.

<sup>‡</sup> L. Eötvös University.